*Materials Science Forum*
*ISSN: 1662-9752, Vol. 1157, pp 9-16*
*doi:10.4028/p-1uGwT1*

*Submitted: 2024-09-19*
*Revised: 2025-02-26*
*Accepted: 2025-02-28*
*Online: 2025-09-05*

# Nitrogen Dopant Incorporation into Epitaxial 4H-SiC and the Influence of CVD Growth Parameters

Alexander Schrader[1,a], Nils Steller[1,b], Dennis Reimann[1,c] and Firas Faisal[1,d*]

[1]Nexperia Germany GmbH, Stresemannallee 101, 22529 Hamburg, Germany

[a]alexander.schrader@nexperia.com, [b]nils.steller@nexperia.com, [c]dennis.reimann@nexperia.com, [d]firas.faisal@nexperia.com

**Keywords:** Epitaxy, CVD, Nitrogen Doping, Dopant Incorporation, Growth Parameters, C/Si Ratio, Site Competition, On-wafer Uniformity

**Abstract.** This study investigates the multifaceted relationships between key process parameters such as C/Si ratio, system pressure, temperature, and growth rate and their effects on nitrogen dopant incorporation in homoepitaxial layers on 4H-SiC substrates. We focus on understanding how these growth parameters influence the in situ nitrogen incorporation during chemical vapor deposition (CVD) of epitaxial layers on 150 mm commercially available SiC substrates. Through a carefully designed experimental framework, which explores the interactions between each parameter and the C/Si ratio, we have shed light on a refined approach for epitaxial growth. This approach may not only stabilize the nitrogen dopant concentration across the wafer but possibly also reduces the formation of epitaxial defects.

**Experimental.** The epitaxial growth was performed consecutively on all wafers using a planetary chemical vapor deposition (CVD) reactor, capable of processing multiple 150 mm SiC wafers simultaneously. The wafers were handled automatically. During operation, all wafers rotate around a central axis, ensuring uniform exposure to the precursor gases. Simultaneously, each wafer rotates individually, driven by a hydrogen/argon gas flow beneath the wafer satellites, promoting homogeneous epitaxial layer deposition. In all epitaxial growth runs, trichlorosilane ($HSiCl_3$), propane ($C_3H_8$), and nitrogen ($N_2$) precursor gases were used with hydrogen ($H_2$) as the carrier gas. Schematics of the reactor design and precursor depletion curves are depicted in Figure 1. The varied growth parameters across different runs included the C/Si ratio, temperature ($T$), system pressure ($p$), total gas flow, growth rate ($GR$), nitrogen gas flow, and growth time. In each epitaxy run, up to eight substrates were processed. Dopant concentrations were measured using capacitance-voltage techniques, epitaxial layer thickness was determined by Fourier-transform infrared (FTIR) spectroscopy, and defect densities were assessed using photoluminescence (PL) and differential interference contrast (DIC) methods. All following data will be shown as percentage deviations from the process of records.

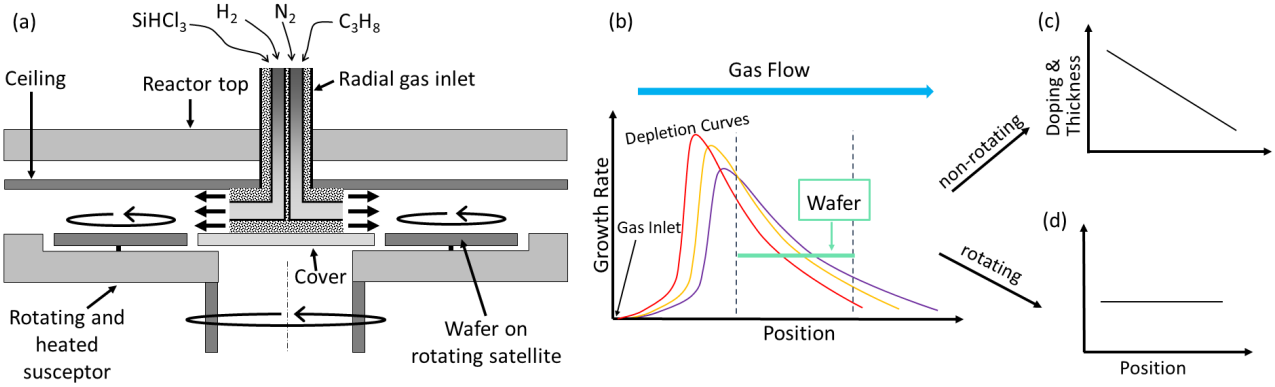


**Fig. 1.** (a) Schematic Illustration of a planetary CVD reactor adapted from [1]. (b) deposition curves of precursor gases and deposition profiles for (c) non-rotating and (d) rotating wafers.

**Pressure Variation.** The influence of system pressure ($p$) on dopant incorporation was investigated as the first CVD parameter. The effect of pressure on nitrogen dopant concentration ([N]) has been extensively reported by numerous research groups [2-7], consistently showing a positive correlation on both Si- and C-face substrates over a wide pressure range (30–1000 mbar) and C/Si ratios. Figure 2 presents the measured data for the doping concentration [N] (light blue) and doping efficiency ($DE$ = [N]/$F_{N_2}$, black) as a function of system pressure.

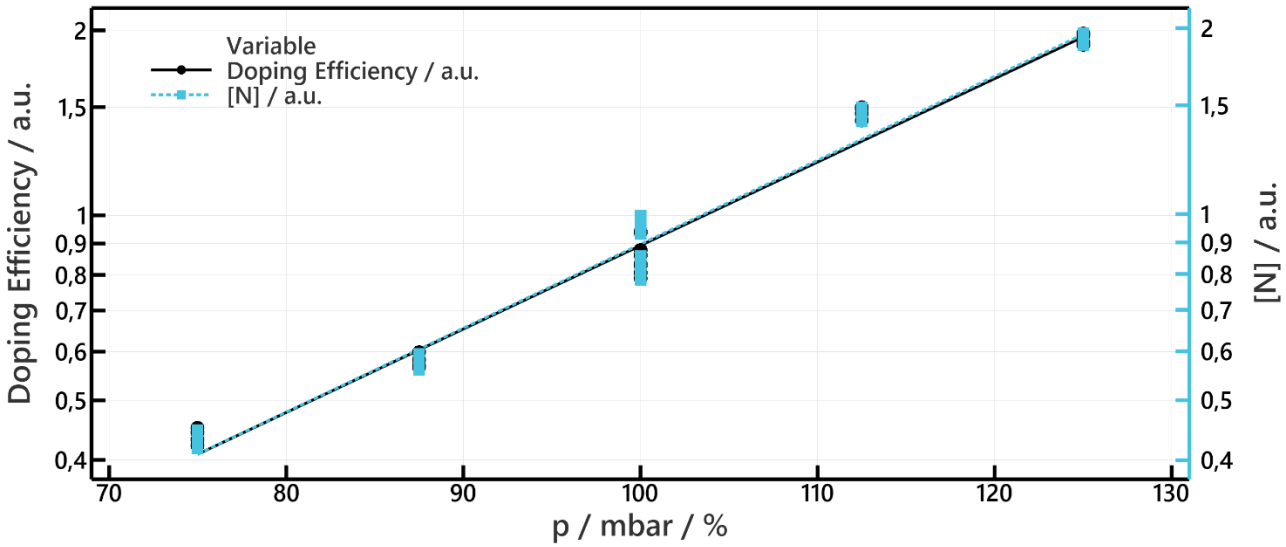


**Fig. 2**. Doping efficiency (*DE)* and N dopant concentration [N] in dependence of *p.* The $N_2$ flow $F_{N_2}$ has been kept constant for all epitaxial runs.

The experimental data for *DE* and [N] were fitted with a linear model, yielding high $R^2$ values of 91.11% and 91.60%, respectively, with slopes of 3.113 and 3.086. These results align well with previous findings from other studies [2-5,7]. The increase in *DE* with system pressure can be explained by a shift in the partial pressure ratio of nitrogen- and carbon-containing precursor species, which are assumed to react at the SiC surface, contributing either an N or C atom to the growing SiC lattice [3]. Forsberg et al. [4], using simulations, proposed that hydrogen cyanide (HCN) and acetylene ($C_2H_2$) are the key gas-phase species for nitrogen and carbon, respectively. Their work demonstrated that the partial pressure ratios $p_{HCN}/p_{C_2H_2}$ and $p_{HNC}/p_{C_2H_2}$ increase with system pressure, thereby altering the effective C/N ratio at the wafer surface. According to the site-competition model [8], this results in enhanced nitrogen incorporation and, consequently, a higher *DE*.

While this interpretation based on shifts in partial pressure ratios, provides a plausible mechanism for the observed pressure-dependence, it remains uncertain whether this is the sole or even the primary process influencing dopant incorporation. Forsberg et al.'s in situ simulations [4] offer valuable insights, yet the absence of a testable fundamental physical model of molecular and atomic dynamics during epitaxial SiC CVD growth leaves room for further exploration. Additional insights into the effects of pressure can be drawn from the on-wafer doping profiles, shown in Figure 3, which may indicate adjacent or contributing phenomena related to system pressure.

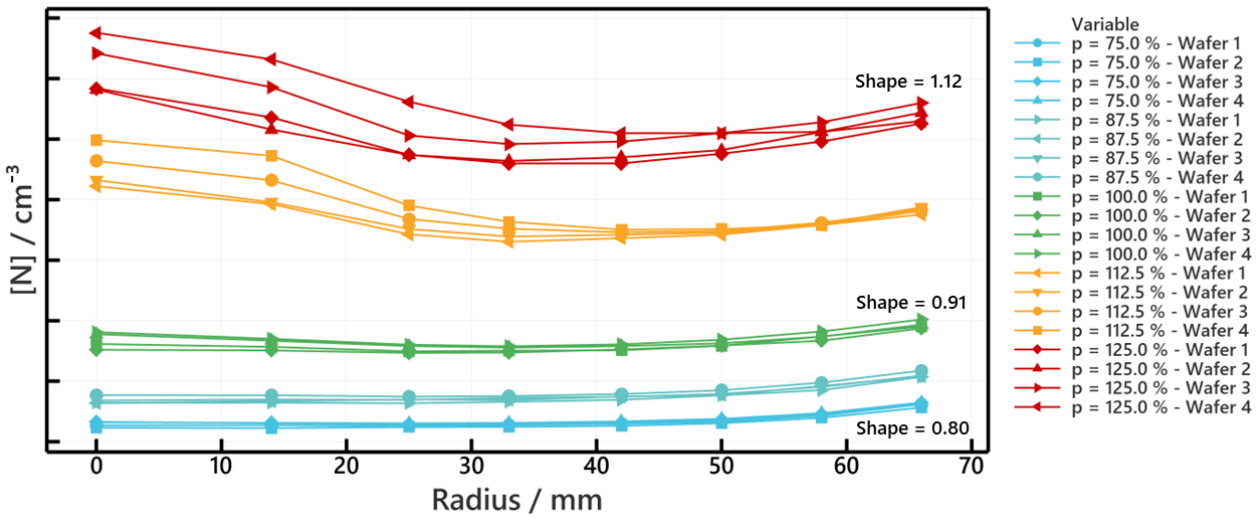


**Fig. 3.** Doping profiles along wafer y-axis at different *p*. The shape factor is the mean average per *p*.

Figure 3 depicts the dopant concentration [N] profiles for the 20 epitaxially grown SiC wafers from Figure 2, plotted along the wafer's y-axis, i.e., from the center point (0, 0) to the wafer edge (0, 68 mm). The data is color-coded, with warmer colors representing higher system pressure (p) and colder colors indicating lower *p*. Two key observations can be derived from these profiles. First, the dopant concentration [N] increases across the entire wafer as the system pressure rises, consistent with the overall trend shown in Figure 2. Second, the shape factor = $[N]_{0mm}/[N]_{68mm}$ of the doping profile changes with increasing *p* and doping efficiency (*DE*). This shape factor is used to quantify the uniformity of dopant distribution across the wafer. A shape factor near 1.00 indicates a more uniform doping profile, whereas deviations from 1.00 suggest a greater disparity between the center and edge concentrations. Here specifically, the increase in [N] is more pronounced near the wafer center than near the edge.

This hints towards a potentially more fundamental effect of varying system pressure on the gas-phase dynamics, not only at the wafer surface but also in the transport and reaction regions between the gas inlet and the wafer. Since system pressure is isotropic throughout the reaction chamber, localized changes in [N] suggest corresponding changes in *DE* at different points on the wafer. These changes may reflect pressure-dependent variations in the site-competition dynamics between nitrogen and carbon. One possible explanation for this behavior is a pressure-induced shift in the maxima and decay tails of the depletion curves for the different precursor gases and their reaction rates, as shown in Figure 1 (b). A shift in these curves could alter the effective C/N ratio at different points on the wafer to a different degree. For example, if the depletion curve for nitrogen-containing species such as $N_2$, HCN, or HNC is shifted further from the gas inlet, or if the tail of the depletion curve for $C_2H_2$ flattens, it could lead to a locally dependent variation in nitrogen incorporation. This modified precursor distribution could explain the observed local differences in dopant concentration change across the wafer, as shown in Figure 2. However, to confirm or refute these interrelationships, further in situ investigations of gas-phase dynamics are required. Such studies could involve either direct experimental measurements or simulations to model the pressure-dependent transport and reaction dynamics in the CVD reactor.

**Temperature Variation.** The next investigated CVD parameter was the growth temperature (*T*). For 4H-SiC Si-face epitaxy, an increase in *T* has been observed to promote nitrogen incorporation, primarily due to enhanced gas-phase reactions of nitrogen-containing precursors (e.g., HCN/HNC) and an increase in carbon vacancies $V_C$ that can be occupied by nitrogen atoms [2-5,7,9]. This behavior is consistent with previous findings, where the availability of $V_C$ increases with higher thermal energy, facilitating nitrogen incorporation. The experimental data supporting this is presented in Figure 4.

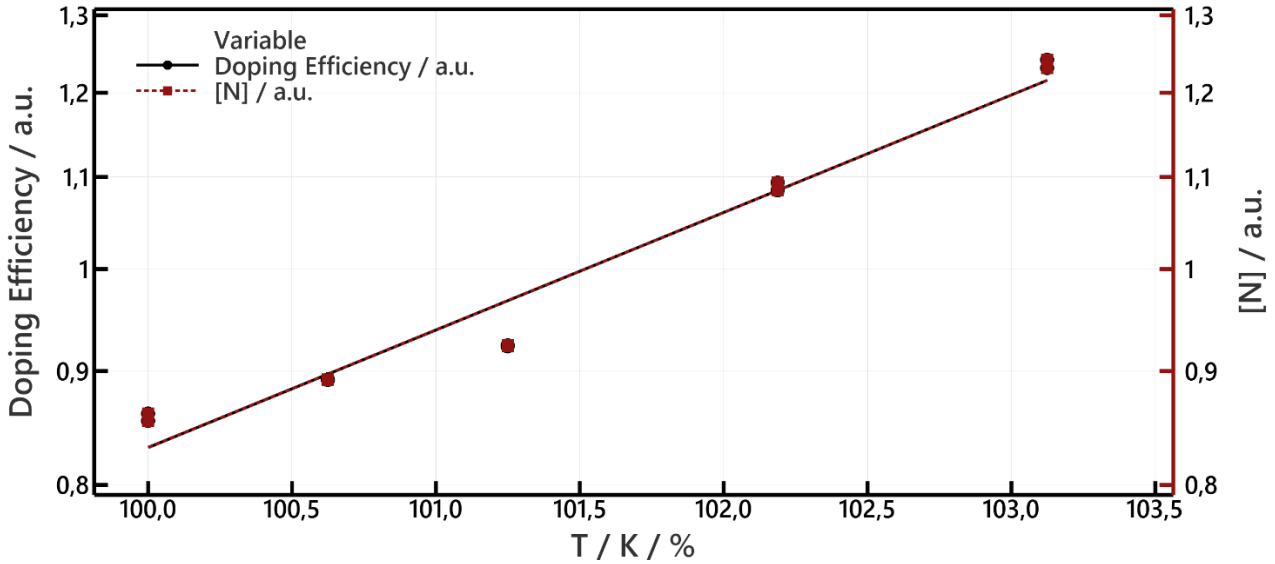


**Fig. 4.** Doping efficiency and N dopant concentration [N] in dependence of *T*.

Our data confirm a positive relationship between *DE*, [N], and *T*, with $R^2$ values of 95.12% for both *DE* and [N], consistent with the literature [2-5,7,9]. Compared to system pressure, the slope of this relationship is ~ 400 % steeper at 12.50 in the transport-limited regime. Due to the sensitivity of the *DE* - T relationship and the constraints of the transport-limited regime, we selected only small temperature variations, all of which were upwards deviations from the standard temperature. Similar to pressure, an increase in *DE* also causes a noticeable change in the doping profile shape with increasing *T*, as seen in Figure 5.

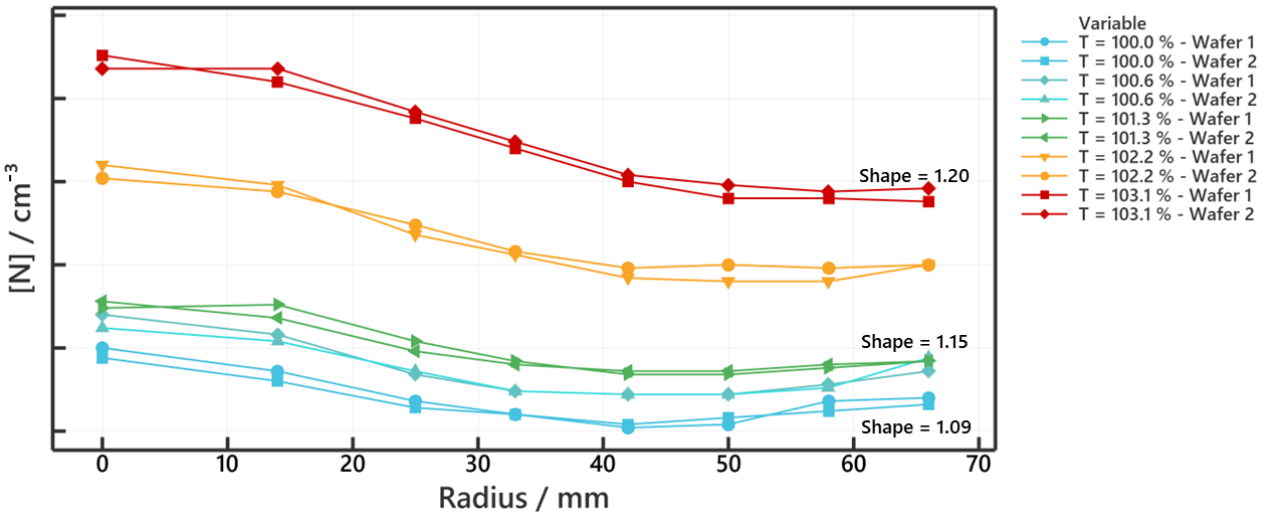


**Fig. 5.** Doping profiles along wafer y-axis at different *T*.

Although the doping profile shape at $T$ = 100% is already greater than 1, it further increases with higher *T*, ranging from 1.09 to 1.20. This is comparatively smaller than the range resulting from pressure variation (0.78 - 1.23). With the wafers at $T$ = 100 % being grown at standard conditions, the doping shape of these wafers would be expected to be around 1.00, which again indicates a highly sensitive and volatile nature of the growth conditions inside of the reaction chamber, heavily influenced by chamber aging effects, loading imperfections and wafer bow.

Given that dopant incorporation, including HCN/HNC precursor synthesis and $V_C$ formation, is at least partially thermally activated, an Arrhenius-type relationship $[N] \propto \exp\left(-\frac{E_A}{R} \cdot \frac{1}{T}\right)$ can be applied to the data from Figure 4. Using this approach, we determined the thermal activation energy $E_A$ to be 52.52 kcal/mol (219.8 kJ/mol). While this value is lower than the 60-260 kcal/mol range reported by

other research groups [2-5,7,9] for C/Si > 1 and Si-face growth, it is still positive, indicating the limiting role of a thermally activated process. A negative activation energy would suggest that thermally activated nitrogen desorption plays a significant role. Simulation studies [9] have proposed that $N_2$ is the primary species contributing to n-type doping, with a triple-bond strength of 226 kcal/mol. However, our determined value for $E_A$ suggests that HCN/HNC may play a more significant role, given their lower formation energy of around 60 kcal/mol [5]. That said, the weakening of the N≡N triple bond upon adsorption to the SiC surface could contribute, so the involvement of $N_2$ should not be entirely ruled out [10].

**Growth Rate Variation.** Following the same variation and measurement scheme as with pressure and temperature, the effect of the growth rate (*GR*) on nitrogen dopant incorporation was investigated. *GR* is primarily determined by the trichlorosilane (TCS) total gas flow into the reaction chamber, as the propane ($C_3H_8$) flow is derived from the TCS flow and the C/Si ratio using the relationship $F_{C_3H_8} = \frac{1}{3} \cdot F_{TCS} \cdot C/Si$ . The relationship between *DE*, [N], and *GR* is shown in Figure 6. Similar to findings by other research groups [4,6], the doping efficiency and, consequently, the doping concentration [N] (at a constant $N_2$ flow) declines rapidly with increasing *GR* on Si-face. Linear fits describe this relationship well, with $R^2$ values of 80.29% and 78.79%, respectively, and slopes of -5.522 and -6.284. While quadratic fits would have yielded higher $R^2$ values, linear fits were chosen to ensure comparability with existing literature. A simulation study by Forsberg et al. [4] suggests that the effective C/Si ratio increases rapidly with $SiH_4$ flow. Their simulations suggest that the concentration of acetylene ($C_2H_2$), which is supposed to be the main C-contributor, increases disproportionately with $SiH_4$ concentration, whereas the concentration of N-containing precursors (HCN/HNC) increases only proportionately (400% increase in $SiH_4$ results in 300% increase in HCN/HNC, but 1600% increase in $C_2H_2$). This phenomenon could be explained by a gas-phase reaction-limited availability of $C_2H_2$, which depends on the gas phase concentration of $SiH_4$ or its byproducts. Our observations suggest a similar behavior in the presence of TCS instead of $SiH_4$, which may be responsible for an increased formation rate of $C_2H_2$. It is not yet clear which exact chemical reaction is the limiting factor here. Nonetheless, our current understanding is that the disproportionate rise in $C_2H_2$ concentration at a constant inlet C/Si ratio leads to an increase in the effective near wafer C/Si ratio. As a result, site competition between carbon- and nitrogen-containing precursors becomes more pronounced, which hinders nitrogen dopant incorporation.

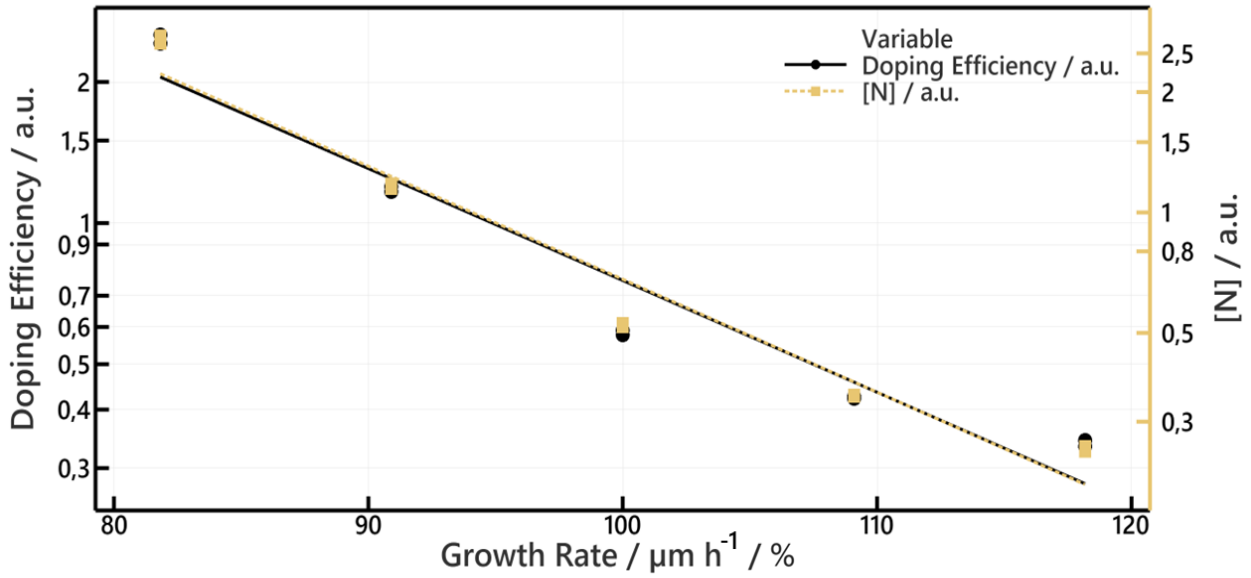


**Fig. 6.** Doping efficiency (*DE)* and N dopant concentration [N] in dependence of *GR*.

The dependence of the doping profile shape on *DE*, previously observed for variations in pressure and temperature, is also observed for variations in growth rate, as shown in Figure 7.

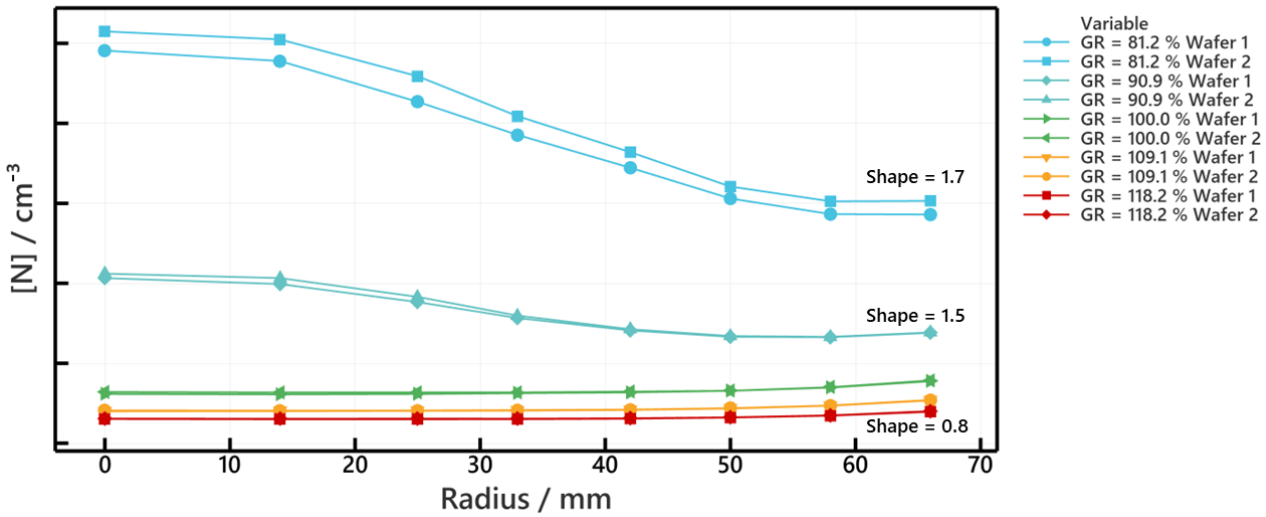


**Fig. 7.** Doping profiles along wafer y-axis at different *GR*.

The observed change in doping profile shape with increasing *DE*, resulting from variations in *GR*, suggests that alterations in the depletion curves of each respective precursor are again at the root of the observed doping profile changes. It is reasonable to assume that with a higher concentration of $C_2H_2$ in relation to other precursors in the gas phase, a larger portion of $C_2H_2$ may not react as early as it would have otherwise. However, to fully clarify which physical mechanisms contribute to these effects, further studies, including in situ measurements and precise simulations, are necessary.

**C/Si Variation at different *p*, *T* and *GR*.** To further investigate the effects of each growth parameter, an additional series of epitaxial growth experiments was conducted at the edge values of pressure (*p*), temperature (*T*), and growth rate (*GR*), while varying the inlet C/Si ratio. A change in the slope of the *DE*–C/Si relationship under different values of the same growth parameter would indicate an alteration to the sensitivity to the inlet C/Si ratio. Specifically, a flatter *DE*–C/Si curve would suggest that dopant incorporation is less sensitive to variations in the effective C/Si. Furthermore, a change in slope would confirm that the influence of the growth parameter is more complex than simply altering the effective C/N ratio. The measured data is presented in Figure 8.

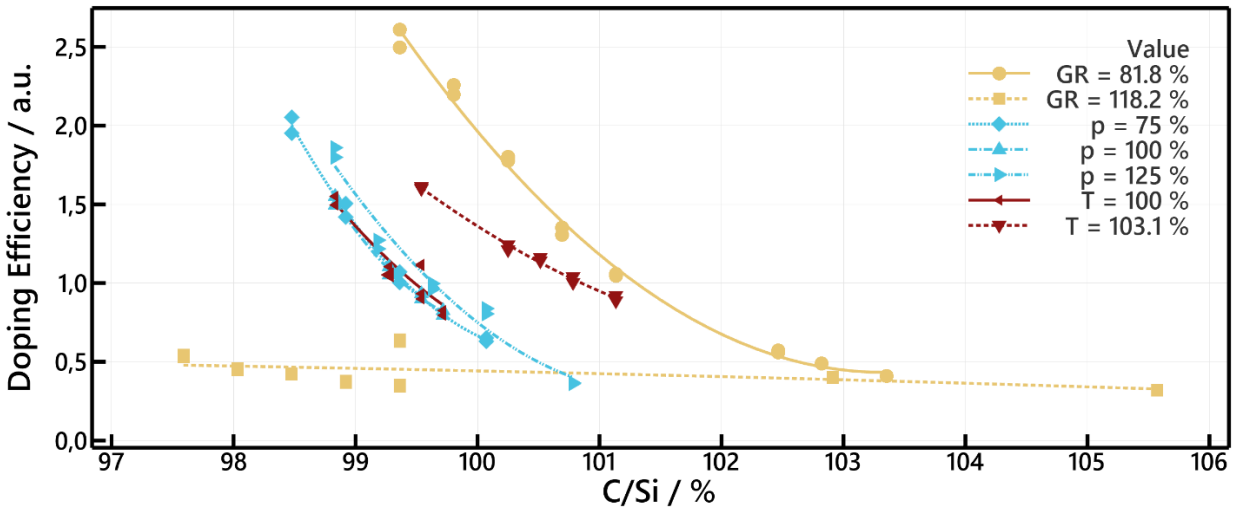


**Fig. 8.** *DE* vs C/Si at extremal values of *p, T* and *GR*.

The data show that variations in *p* do not affect the curvature of the *DE*–C/Si curve, whereas changes in *T* and *GR* result in moderate to significant changes. In the case of pressure variation, the mechanism proposed by Forsberg et al. [4], where an increased system pressure leads to an increased partial pressure ratio between N- and C-containing precursors (i.e., $p_{HCN}/p_{C_2H_2}$ and $p_{HNC}/p_{C_2H_2}$), is expected to only modify the effective C/Si and, consequently, the effective C/N ratio. Our observation

of no change in the curvature of the *DE*–C/Si curve at different pressures supports this hypothesis, affirming that the dominant effect of increased pressure on nitrogen incorporation is the partial pressure ratio shift.

In contrast, temperature variation shows a noticeable flattening of the *DE*–C/Si curve at elevated *T*. According to Ferro et al. [2,3], the effect of *T* can be attributed to two distinct mechanisms, both related to carbon etching via $H/H_2$. First, the etching of carbon atoms from the SiC surface or lattice reduces the effective C/Si and C/N ratios, which promotes nitrogen incorporation. Second, the formation of carbon vacancies $V_C$ creates binding sites for nitrogen atoms, which also enhances dopant incorporation. However, the formation of $V_C$ is independent of the inlet or effective C/Si ratio. While the C/N ratio influences which atoms occupy $V_C$, the creation of additional nitrogen-binding sites generally promotes nitrogen adsorption, regardless of the presence of C-atoms. Since this second effect is independent of the C/N ratio, a flatter *DE*–C/Si curve was expected at higher temperatures, as the increase in *DE* is not solely due to reduced site competition.

Growth rate (*GR*) exhibits the most significant impact on the curvature of the *DE*–C/Si curve. At an increased *GR* (~ 118 %), the curve becomes almost flat, while at a reduced *GR* (~ 81 %), the curvature is similar to that of standard conditions ($p$ = 100 % in Figure 8). Multiple factors likely contribute to this behavior. As previously mentioned, an increased TCS and propane flow rate (which drives *GR*) increases the reaction rate of $C_2H_2$ more than the formation of HCN/HNC, thereby modifying the C/N ratio to the disadvantage of nitrogen incorporation. Additionally, the prevention of nitrogen desorption due to an increased influx of atoms from the gas phase could explain the divergent responses to *GR* changes between the C-face and Si-face. While higher *GR* promotes nitrogen incorporation on the C-face, it decreases incorporation on the Si-face. This suggests that nitrogen desorption plays a more prominent role on the C-face than on the Si-face, as demonstrated by Ferro et al.'s vacancy exchange model [2,3]. In this model, C-sites on the Si-face are shielded by an overlayer of Si-sites, whereas the opposite is true on the C-face. While the stark contrast in curvature of the *DE*-C/Si curves at higher and lower *GR*s hints towards a possible significance of thermal N desorption from Si-face, the positive $E_A$ of 52.52 kcal/mol from Figure 4 would be contradictory. The increased independence of the *DE* from the inlet C/Si at higher growth rates could further indicate an inherent limitation of the availability of TCS, propane or its byproducts at standard conditions, which are necessary for the formation of $C_2H_2$. With such an increase in the abundance of a limiting key molecule for epitaxial SiC growth and/or the incorporation of dopant atoms, an independence from the inlet C/Si would be plausible while remaining in C-rich environments.

**Summary**

This study investigates the effects of key chemical vapor deposition process parameters as system pressure, temperature, growth rate, and C/Si ratio on nitrogen dopant incorporation in SiC epitaxy. The results demonstrate that increased system pressure and temperature promote nitrogen incorporation, while an elevated growth rate reduces doping efficiency. These trends are primarily driven by changes in the effective C/Si ratio near the wafer surface, which alters the balance between nitrogen and carbon incorporation due to site competition. Variations in the C/Si ratio interact differently with each parameter, affecting dopant distribution and defect formation.

This study provides a refined understanding of the interplay between growth conditions and dopant incorporation, offering insights for optimizing epitaxial growth processes for SiC. The findings highlight that optimizing these parameters can potentially lead to a more uniform dopant concentration profile across wafers, improving the quality of SiC substrates. However, further investigation is required to assess how these adjustments impact defect densities, such as stacking faults and pit defects, which could influence the performance of SiC-based electronic components. Additionally, understanding the molecular dynamics during epitaxial growth, including gas-phase reactions and precursor interactions with the SiC lattice, is essential. Future research using advanced

simulation models or in situ measurements will be critical in refining epitaxial growth processes on commercially available 4H-SiC wafers.

**References**

[1] F. Yang, Modern Metal-Organic Chemical Vapor Deposition (MOCVD) Reactors and Growing Nitride-based Materials, in Nitride Semiconductor Light-Emitting Diodes (LEDs), Elsevier, 2014, pp. 27–65.

[2] G. Ferro and D. Chaussende, A New Model for in situ Nitrogen Incorporation into 4H-SiC during Epitaxy, Scientific Reports 7 (2017) 43 069.

[3] G. Ferro and D. Chaussende, Revisiting the Site-Competition Doping of 4H-SiC: Cases of N and Al, Materials Science Forum, Trans Tech Publ Ltd 1004 (2020) 96–101.

[4] U. Forsberg, O. Danielsson, A. Henry, E. Janzen, Nitrogen Doping of Epitaxial Silicon Carbide, Journal of Crystal Growth 236 (2002) 101–112.

[5] H. Saitoh, A. Manabe, T. Kimoto, Epitaxial Growth of 4H-SiC {0001} with Large Off-Angles by Chemical Vapor Deposition, Materials Science Forum, Trans Tech Publ Ltd 527–529 (2006) 223–226.

[6] M. Zielinski, R. Arvinte, H. Peyre, p-type Doping of 4H- and 3C-SiC Epitaxial Layers with Aluminum, Materials Science Forum, Trans Tech Publ Ltd 858 (2016) 137–142.

[7] J. Zhang, A. Ellison, A. Henry, E. Janzén, Nitrogen Incorporation during 4H-SiC Epitaxy in a Chimney CVD Reactor, Journal of Crystal Growth 226 (2001) 267–276.

[8] D. J. Larkin, P. G. Neudeck, L. G. Matus, Site-Competition Epitaxy for Superior Silicon Carbide Electronics, Applied Physics Letters 65 (1994) 1659–1661.

[9] Ö. Danielsson, U. Forsberg, E. Janzén, Predicted Nitrogen Doping Concentrations in Silicon Carbide Epitaxial Layers Grown by Hotwall Chemical Vapor Deposition, Journal of Crystal Growth 250 (2003) 471–478.

[10] J. Olander, K. M. E. Larsson, Adsorption of N-containing Species onto SiC(0001) Surfaces: A Theoretical Study, Physical Review B - Condensed Matter and Materials Physics 67 (2003) 115306.